

Effect of Recycled Aggregate on the Compressive Behaviour of Short Concrete Columns

Hasan Hastemoglu*

Suleyman Demirel University, Isparta, Turkey

Abstract

In this study, 12 specimens with three different lateral reinforcement ratios ($\rho=0.022$, 0.012 and 0.007) and four RG replacement ratios (0%, 30%, 50% and 100%) were prepared and tested under pure axial load in order to investigate the influence of recycled coarse aggregate (RG) and lateral tie reinforcement ratio (ρ) on the compressive behavior of a confined recycled aggregate concrete (RAC) column. The experimental data obtained from the tests are reported and compared with the predicted values obtained from the widely accepted Mander's confined concrete model developed for conventional confined concrete to assess applicability of the model to recycled aggregate concrete. The results showed that the effect of RG on the compressive behavior of the RAC was negligible at low stress level, and it began to appear as the load increased at load levels above about 35% of Peak, regardless of ρ . The slope of the normalized compressive strength (f_{cc_exp}/f_{cc_model}) and normalized corresponding strain ($\epsilon_{cc_exp}/\epsilon_{cc_model}$) against ρ showed that the lateral reinforcement exerted the greatest effect on the stress and strain enhancement in the RG-30 series, and the smallest effect in the RG-50 series. The ratios of experimental values to those predicted from Mander's model, f_{cc_exp}/f_{cc_model} and $\epsilon_{cc_exp}/\epsilon_{cc_model}$ showed that the model tended to give unconservative strength (f_{cc}) and strain (ϵ_{cc}) values for the RAC columns.

Keywords: Concrete; Columns; Confined concrete; Recycled aggregate; Reinforcement

Introduction

The need to recycle old construction materials has been well established over the last few decades by government agencies and the construction industry due to the increasing cost of waste storage and the depletion of natural resources [1]. Among the numerous construction waste materials, old concrete, in particular, is a promising source of recycled aggregate with sufficient quality for civil engineering applications with moderate performance requirements [2,3]. While most of the studies on the subject thus far have focused on the processing of old concrete and the properties of recycled aggregate concrete (RAC), only a limited number of studies have reported the performance of structural members made of RAC: beam [4-6], column [7], joint [8], and frame [9]. Although a direct comparison of the results from different studies is difficult due to a lack of coherent concrete constituents, the results generally indicate that the strength decreases with slight increase in the corresponding strain as recycled aggregate content in the concrete increases. This strength decrement was attributed to a weak interface between the new mortar and the recycled aggregate and between the adhered mortar and the recycled aggregate [10,11]. The reduction in strength due to RG can be offset by two approaches: adjusting proportions of concrete constituents or providing proper reinforcement. The choice between the two approaches should be made based on the required structural performance and cost. Low tensile-high compressive strength cementitious materials typically exhibit brittle behavior, but their ductility and compressive strength improves significantly when subjected to favorable biaxial pressure [12]. For the past few decades, the compressive behavior of concrete confined by properly arranged lateral reinforcements has been extensively studied by many researchers. The effects of various parameters, including concrete strength, amount of lateral reinforcement, lateral reinforcement configuration, dimensions, and cross section geometry, on confined concrete behavior are now sufficiently understood. As a result, the use of confined concrete columns has become a common practice for seismic resistant design [13]. Nevertheless, as aforementioned, most of the confined concrete studies focused on concrete containing virgin aggregate. Recently, the performance of reinforced RAC frame, which satisfies the requirement

set by the ACI earthquake resistant design code and the Chinese standard, has been reported by Xiao et al. [9]. Although Xiao's test demonstrated the potential use of reinforced recycled aggregate in the seismic resistance frame, few studies have investigated the effect of recycled aggregate on confined concrete members, of which behavior is critical for modern, high performance design. Hence, in an attempt to broaden the use of RAC, the influences of the recycled coarse aggregate (RG) content and the volumetric ratio of lateral reinforcement on the compressive behavior of confined columns subjected to concentric load are experimentally investigated here. In addition, the applicability of the existing design model [14] is assessed against the experimental results.

Experimental Program

Materials

River sand and crushed gravel were used as natural fine (NS) and natural coarse aggregate (NG), respectively. The recycled coarse aggregate (RG) was obtained from 5 concrete (at least 20 years old, with a typical design compressive strength of $18 \sim 20$ MPa) collected from an apartment redevelopment site in Korea. The RG was separated from the cement matrix through multiple crushing stages while the loose fine particles were washed off the surface of the RG to minimize the effect of the fines generated during the crushing [15]. The resulting RG only contained small amounts of adhered old mortar and had similar physical properties to those of the NA, as shown in Table 1. The RG used in this study meets the Korean Industrial Standard KS F

*Corresponding author: Hasan Hastemoglu, Suleyman Demirel University, Faculty of Architecture 32260, Isparta, Turkey, Tel: +90 246 2118259; E-mail: hasanhastemoglu@sdu.edu.tr

Received October 12, 2015; Accepted October 23, 2015; Published November 05, 2015

Citation: Hastemoglu H (2015) Effect of Recycled Aggregate on the Compressive Behaviour of Short Concrete Columns. J Civil Environ Eng 5: 194. doi:[10.4172/2165-784X.1000194](https://doi.org/10.4172/2165-784X.1000194)

Copyright: © 2015 Hastemoglu H. This is an open-access article distributed under the terms of the Creative Commons Attribution License, which permits unrestricted use, distribution, and reproduction in any medium, provided the original author and source are credited.

2573 for recycled aggregate for structural concrete use. For the binder, locally manufactured, Type I Portland cement satisfying ASTM C150 specifications was chosen for the concrete mix (Table 1).

Concrete mixes were prepared by replacing NG with RG at four different replacement ratios of 0%, 30%, 50% and 100% as shown in Table 2. The amounts of high performance water reducing admixture (polycarboxylic acid type) and air entraining agents (neutralized vinsol resin type) were adjusted to achieve the target slump and air content of 200 mm and 6% respectively. The average compressive strength of the control concrete the tests was 30 ~ 34 MPa (Table 2).

For each steel reinforcement bar size, three steel samples were tested under tension. The average yield strength, yield strain, Young's modulus values from the test, and specified ultimate strength of the steel rebar are given in Table 3.

Column specimens

A total of 12 specimens of concrete columns were prepared with three different lateral reinforcement ratios ($\rho=0.022$, 0.012, and 0.007) and the four different RG replacement ratio. The tie hoop spacing was set at 30 mm ($\rho=0.022$), 65 mm ($\rho=0.012$) and 100 mm ($\rho=0.007$) to satisfy the minimum tie hoop spacing specified by the two standards: D/2 (100 mm), based on the earthquake-resistant design of the Architectural Institute of Korea; and D/4 (50 mm), based on the earthquake-resistant design of the ACI Committee 318-05. The details of the test specimens are listed in Table 4, and the detailed dimensions of the column specimens are illustrated in Figure 1. All the specimens shared the same dimensions of 200 mm \times 200 mm cross section and 600 mm height. The upper and lower 100 mm of the specimens along the length were reinforced internally with tie hoops spaced at 20 mm and fitted externally with a carbon fiber reinforced plastic wrap to

Type	Max	Specific gravity	Water absorption	Fineness modulus	Bulk density (kgf/m ³)
NG		2.6	1.63	6.52	1642
RG	25	2.48	1.93	6.77	1615
NS	5	2.53	1.62	2.79	1455

Table 1: Physical properties of aggregates.

Specimen	W/C	S/A	AD	Unit Weight (N/m ³)		Slump	Air content (%)
	%	%	% W	C	NGRG	NS(mm)	
RG-0-30				983.7	0	205	5.5
RG-0-65							
RG-0-100							
RG-30-30				688.6	301.1	200	5
RG-30-65							
RG-30-100							
RG-50-30	50	42	0.6	175	350	726.7	
RG-50-65				491.9	501.8	195	6.5
RG-50-100							
RG-100-30				0	1003.5	190	6
RG-100-65							
RG-100-100							

Table 2: Mix proportions and wet concrete properties.

Type	Fyh (MPa)	Es (GPa)	$\epsilon_y (\times 10^{-6})$	Fsu (MPa)
D13	420	183	2,945	630
D6	324	240	2,365	590

Table 3: Mechanical properties of deformed steel bars.

Specimen	Section (mm)	Tie hoop		Longitudinal rebar ratio
		Spacing	Volumetric ratio	
RG-0-30	200 \times 200	30	0.012	8-D13 -0.025
RG-0-65		65	0.006	
RG-0-100		100	0.004	
RG-30-30		30	0.012	
RG-30-65		65	0.006	
RG-30-100		100	0	
RG-50-30		30	0	
RG-50-65		65	0.006	
RG-50-100		100	0.004	
RG-100-30		30	0.012	
RG-100-65		65	0.006	
RG-100-100		100	0.004	

Type of aggregate: RG (Recycled aggregate)

Replacement ratio of RGs: 0 (:0%), 30 (:30%), 50 (:50%), 100 (:100%)

Tie hoop spacing: 30 (:30 mm), 65 (:65 mm), 100 (:100 mm)

Table 4: Column specimens.

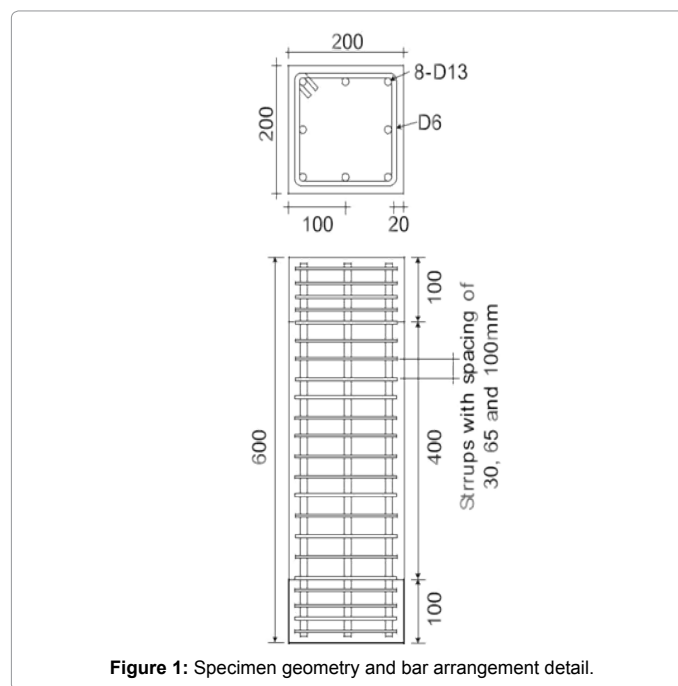
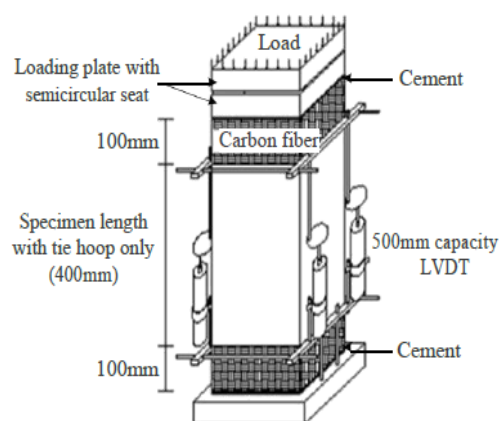


Figure 1: Specimen geometry and bar arrangement detail.

prevent the bearing failure of the specimen ends prior to failure of the test area of the specimens (Table 4 and Figure 2). The tie hoops were made of D6 (6 mm nominal diameter) rebar and one D13 (13 mm nominal diameter) longitudinal rebar was placed at each corner of the column. The hooks of the tie hoops were anchored with 135° bending, with an extended length of 6db, which is longer than the minimum length required by the ACI Code. The cover depth of concrete from the center of the tie hoops was 17 mm, and the cross section of the core surrounded by the center of a tie hoop was 166 mm \times 166 mm. The ratio of the core area to the entire cross section was fixed at 69% for all specimens.

Test setup and measurement

A square plate with a semicircular seat was placed on the top of the specimen to prevent any moment load on the specimen by eccentric load prior to application of the axial load. The loading was



Schematic illustration of loading test and specimen

Figure 2: Test set up method: (a) Schematic illustration of loading test and specimen.

Specimen	f'_{co} (MPa)	Pcr (kN)	ϵ_{cr}	Ppeak (kN)	ϵ_{cc}
RG-0-30	34.1	1,190	0.00245	1816	0.00476
RG-0-65		1,110	0.00282	1712	0.00382
RG-0-100		1,086	0.00138	1675	0.00339
RG-30-30	33.5	1,150	0.00214	1815	0.00495
RG-30-65		1,050	0.00121	1638	0.00347
RG-30-100		976	0.00153	1538	0.00325
RG-50-30	32.4	1,029	0.00188	1785	0.00499
RG-50-65		1,009	0.001	1738	0.00368
RG-50-100		882	0.00121	1677	0.00372
RG-100-30	30.5	999	0.00146	1727	0.00453
RG-100-65		985	0.00126	1622	0.00375
RG-100-100		701	0.00078	1582	0.00326

Table 5: Test results.

applied under load control such that the initial rate of displacement was about 0.30 mm/min, equivalent to 0.00075 strain/min. As load increased the loading rate was carefully adjusted in order to trace the unloading part of the curves. The loading was stopped when the post-peak descending curve shape became apparent or when stable loading could no longer be attained. The deformation measurements were recorded at constant time intervals using a data logger (TML TDS-303). The axial deformation of the specimen was recorded from the four linear variable differential transducers (LVDT) installed at each corner of the specimen. The average deformation value from the four LVDTs was calculated and used as the axial deformation value. We note here that the fixtures with vertical rigid rod with horizontal end plate placed above the LVDTs were attached to the top of the specimen in order to measure compressive deformation over the entire length of the specimen.

Results and Discussion

Failure modes

The maximum (Peak) and critical (Pcr) loads at which significant cover spalling occurred are listed in Table 5. The first visible crack appeared in a vertical direction near a corner edge at 60 ~ 80% of Peak, as the cover concrete deterioration worsened, and Ppeak

was reached at a strain much greater than those of the unconfined concretes. Subsequently, with further increase in the applied load, the cover concrete of the specimens began to spall. For a given tie hoop spacing, the rate of cover concrete spalling was proportional to the RG replacement ratio (Figure 3).

After localized crack damage was observed on a side of the column, notable spalling of the cover concrete occurred with a gradual decrease in the applied load. Spalling of the cover concrete occurred at a lower applied load in RAC than in natural aggregate concrete (NAC). The lower Pcr of RAC can be attributed to the relatively higher water absorptiveness of RG, which should have created a steeper moisture content gradient from the cover layer to the interior layer of the specimen. In turn, the moisture content gradient due to RG can cause higher incompatible drying shrinkage between the interior and exterior RAC, compared to that of NAC [16], thereby facilitating the cover was spalling. Furthermore, the lower bond strength between the rebar and RAC than NAC [17] also contribute to the lower cover spalling load and the faster rate of cover degradation in RAC compared to those of the NAC columns.

Compressive stress-strain curves

Stress-strain curves of the plain concrete cylinders with different RG contents up to the maximum stress are shown in Figure 3. The curves show a greater loss of stiffness at a given load level with increasing RG replacement ratio. The effect of RG on the compressive behavior of concrete became apparent at about 10 MPa, which is 31% of the average strength of the four specimens, similar to the result reported by Topcu IB, et al. [18]. The axial compression tests of the laterally reinforced RAC columns showed that their compressive behavior in almost entire strain range, both the ascending and descending branches of the stress-strain curve, is affected by the RG, as shown in Figure 4. In all the specimens, the ascending branch of the stress-strain curves of the column containing RG showed a smaller increase in stress per given strain increase than that of the concrete column containing NA only, and the Ppeak value of the RAC column was lower than that of the NAC column. The lower stiffness of RAC compared to that of NAC can be attributed to presence of micro-

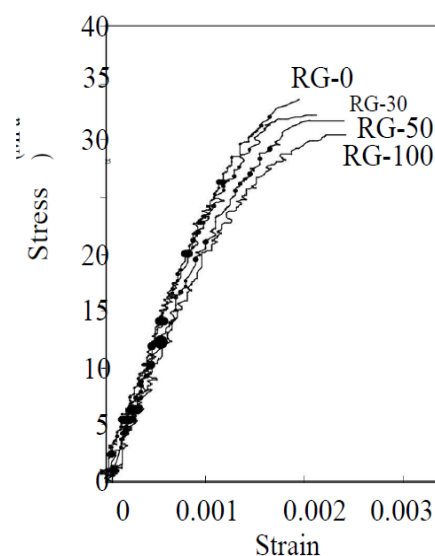


Figure 3: Stress-strain curve of unconfined concrete cylinder with different RG content.

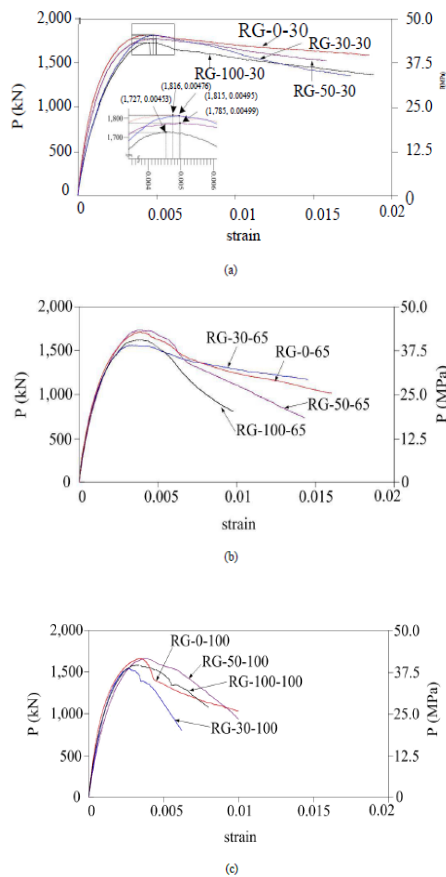


Figure 4: An axial load-strain curve of RAC column: tie hoop spacing (a)=30 mm, (b)=65 mm, and (c)=100 mm.

cracks in the RG and adhered mortar on the RG surface [19,20]. At low load below 600kN (15MPa), the specimens having the same tie hoop spacing showed almost identical compressive behavior, regardless of the RG replacement ratio. However, the compressive behavior of the specimens with different RG replacement ratio began to diverge with increasing load. In the descending branch, the shape of the curves indicated that the effect of the RG content on the post-peak behavior of the column was diminished by the lateral reinforcement as the ρ ratio increased: steady curves were recorded from the RG-X-30 series which showed a gentler slope with less RG content, while curves with abrupt change in slopes were recorded from the RG-X-65 and the RG-X-100 series. In case of RG-X-30 series, the specimens shown similar ductility effects until strain 0.03 regardless of RG replacement ratio, but in case of RG-X-65 series, the ductility effects of RAC declined than that of the RG-0-65(0.016) as the minimum 0.0098(RG-100-65) and the maximum 0.0132(RG-30-65) with increasing of RG replacement ratio. In the RG-X-100 series, the strain value of RAC declined than that of RG-0-100(0.095) as the minimum 0.0062(RG-30-100) and the maximum 0.0069(RG-50-100), and it was failure more quickly than RG-0-100 specimen. The steepness of the descending curves of the test specimens should correspond to the rate of concrete deterioration mentioned earlier (Figure 4).

Effect of lateral tie reinforcement ratio (ρ) on the confined RG concrete strength and the corresponding strain

The effect of ρ on the confined RAC behavior was examined by

comparing the slope of the normalized compressive strength (f_{cc}/f_{co}) and of the normalized corresponding strain ($\epsilon_{cc}/\epsilon_{co}$) with increasing ρ . Figure 6 shows that, for all four RG contents, the strength and strain enhancements of concrete were proportional to ρ . The slopes of the fitted curve in Figure 5a indicated that the effect of lateral reinforcement on the strength enhancement was greatest in the RG-30 series, followed in order by RG-100, RG-0, and RG-50. Similarly, the slopes of the fitted curve in Figure 5b indicated that ρ exerted the greatest effect on the strain enhancement in the RG-30 series, followed in order by RG-50, RG-0, and RG-100. Although the fitted curves of the RAC showed variations in strength and strain enhancement by lateral reinforcement from those of NAC, the confinement seemed to be effective regardless of the RG replacement ratio over all. For a fixed ρ , the strength enhancement due to the tie hoops seemed to increase with increasing RG content (at $\rho=0.004$; $f_{cc}/f_{co}=1.35$ (RG-30), $f_{cc}/f_{co}=1.38$ (RG-50), $f_{cc}/f_{co}=1.42$ (RG-100)). Similarly, the strain enhancement tended to increase with increasing aggregate content (at $\rho=0.006$; $\epsilon_{cc}/\epsilon_{co}=1.48$ (RG-30), $\epsilon_{cc}/\epsilon_{co}=1.53$ (RG-50), $\epsilon_{cc}/\epsilon_{co}=1.59$ (RG-100)) (Figure 6).

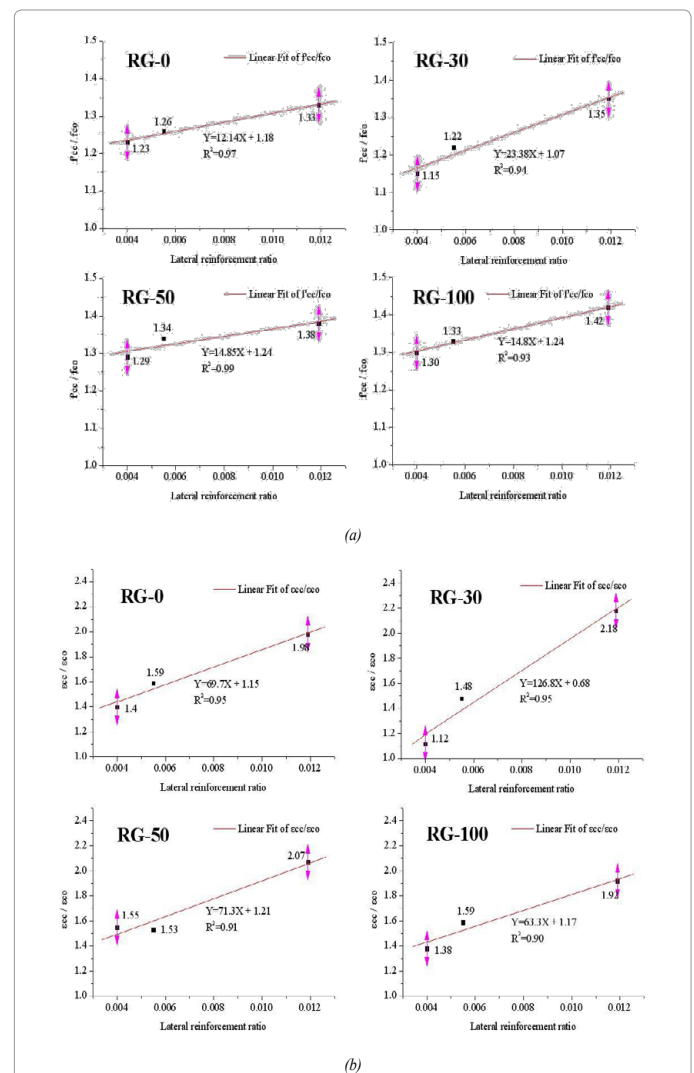


Figure 5: Effect of lateral reinforcement ratio (ρ) on the enhancement of (a); f_{cc} and (b); ϵ_{cc} with different recycled aggregate contents.

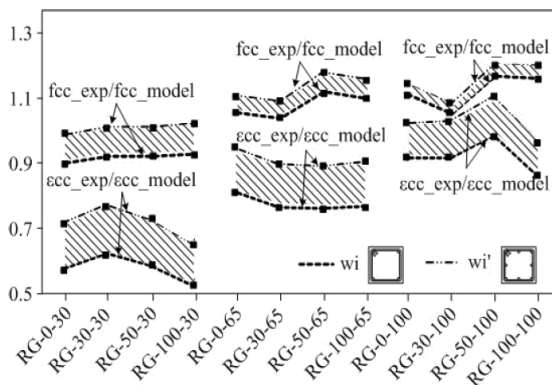


Figure 6: Comparison between experimental values and those predicted by the modified and existing Mander's model.

Comparison between the test results and values predicted by the existing confined NAC model

To assess the applicability of the existing compressive confined concrete model to the confined RAC, the experimental values of the confined RAC concrete's compressive strength (f'_{cc_exp}) and corresponding compressive strain (ϵ_{cc_exp}) at f'_{cc_exp} were compared with the values predicted by the existing model. Mander's model, equations (1) through (3), was selected as it is widely used in practice and in research.

The confinement effectiveness coefficient (k_e) value in Equation (3) was calculated according to the method suggested for rectangular concrete sections confined by rectangular hoops with or without cross tie by Mander et al. [14].

$$f'_{cc} = f'_{cc} \left(2.254 \sqrt{1 + \frac{7.94 \cdot f'_l}{f'_{cc}}} - \frac{2 \cdot f'_l}{f'_{cc}} - 1.254 \right) \quad (1)$$

$$\epsilon_{cc} = \epsilon_{co} \left[1 + 5 \left(\frac{f'_{cc}}{f'_{co}} - 1 \right) \right] \quad (2)$$

$$f'_l = k_e \rho f_{yh} \quad (3)$$

Where, f'_{co} =compressive strength of unconfined concrete; ϵ_{co} =compressive strain of unconfined concrete at f'_{co} ; f'_{cc} =compressive strength of confined concrete; ϵ_{cc} =compressive strain of confined concrete at f'_{cc} ; f_{yh} =yield strength of lateral reinforcement; k_e =confinement effectiveness coefficient; ρ =volumetric ratio of transverse steel reinforcement. The ratios of the experimental values to those predicted from the existing model, $f'_{cc_exp}/f'_{cc_model}$ and $\epsilon_{cc_exp}/\epsilon_{cc_model}$, are shown in Table 6. The average $f'_{cc_exp}/f'_{cc_model}$ and $\epsilon_{cc_exp}/\epsilon_{cc_model}$ were 0.98 and 0.79, with standard deviation of 0.069 and 0.065, respectively. These results indicated that the existing Mander's model gave the unconservative strength (f'_{cc}) and strain (ϵ_{cc}) values for the RAC columns. This may be explained the fact that as Mander's model was originally developed to predict the confined strength and corresponding strain of normal concrete made of natural aggregates, it therefore does not account for different RG replacement ratio in conjunction with different ρ . The discrepancy observed between the predicted and experimental values is in agreement with

Van Mier [21] and Shah and Ahmad [22], who stated that it is not sufficient to determine the mechanical behavior of confined concrete by parameters such as concrete strength, yield strength and volumetric ratio of the confining reinforcement. The importance of aggregate type was also reported by El-Dash and Ramadan [23], who found that the aggregate type influences the behavior of confined concrete, especially the roundness of the aggregate which assists to distribute the lateral confinement pressure and helps the concrete element to resist higher stress than the angular aggregate. Therefore, as well as the parameters noted above, the type of aggregate and its content shall also be considered in the model (Table 6). The existing model reasonably estimates the compressive strength of the RAC columns with the lateral reinforcement is shown in Figure 6. The average ratio of $f'_{cc_exp}/f'_{cc_model}$ was 0.92, 1.01, and 1.04 for hoop spacing of 30 mm, 65 mm, and 100 mm, respectively. However, when the strain at f'_{cc} is considered, Figure 6 clearly shows that the existing model overestimates the ϵ_{cc} value by an average of 25%, 20% and 20% with 30 mm, 65 mm and 100 mm respectively. In general, the existing equations (1) – (3) tend to overestimate the confined effect of RAC with increasing tie hoop spacing, which renders the existing Mander's model unconservative for use in the design of RAC, especially with high lateral reinforcement. Therefore, the model needs to be modified. Also the $f'_{cc_exp}/f'_{cc_model}$ and $\epsilon_{cc_exp}/\epsilon_{cc_model}$ ratios are proportional to the RG content at a tie hoop spacing of 30 mm. However, this proportionality was no longer evident as the tie hoop spacing was increased to 65 mm and 100 mm, indicating that the existing model can only be successfully modified by considering effect of ρ that is dependent on the RG replacement ratio.

Conclusions

Based on the results of the RAC compressive test and comparison between the test results and the values predicted by the existing model, the following conclusions were drawn:

(1) The effect of RG on the compressive confined RAC column was negligible in the ascending branch of the load-strain curve up to 600 kN, which was 35% of the average confined strength of all specimens tested.

(2) Examination of the stress-strain curves indicated that the influence of the RG content increased in both the ascending and descending branches of the stress-strain curves with decreasing ρ .

(3) The ratios of the experimental values to those predicted from the existing model ($f'_{cc_exp}/f'_{cc_model}$) ranged from 1.00 to 1.12, and the $\epsilon_{cc_exp}/\epsilon_{cc_model}$ ratio from 1.00 to 1.16. The existing Mander's model tended to give unconservative strength (f'_{cc}) and strain (ϵ_{cc}) values for the RAC columns.

Specimen	Confined strength f'_{cc} (MPa)			Confined strain ϵ_{cc} (MPa)		
	Exp.	Model	Exp./Model	Exp.	Model	Exp./Model
RG-0-30	45	43.764	1.04	0.00476	0.006377	0.75
RG-0-65	43	38.757	1.1	0.00382	0.005462	0.7
RG-0-100	41.88	37.203	1.13	0.00339	0.005136	0.66
RG-30-30	45	43.148	1.05	0.00495	0.006293	0.79
RG-30-65	41	38.153	1.07	0.00337	0.004794	0.7
RG-30-100	38.45	36.601	1.05	0.00255	0.003947	0.65
RG-50-30	44.63	42.017	1.06	0.00499	0.006928	0.72
RG-50-65	43.45	37.046	1.17	0.00368	0.006493	0.57
RG-50-100	41.93	35.497	1.18	0.00372	0.005928	0.63
RG-100-30	43.18	40.059	1.08	0.00453	0.007233	0.63

Table 6: Comparison of experiment results to those of the existing model.

References

- Poon CS, Chan D (2007) The use of recycled aggregate in concrete in Hong Kong. *Resources Conservation and Recycling* 50: 293-305.
- Hansen TC (1986) Recycled aggregate and recycled aggregate concrete 2nd state-of-art report development from 1945-1985. *Mater Struct* 19: 201-246.
- ACI Committee 555 (2002) Removal and reuse of hardened concrete. *ACI Mater J* 99: 300-325.
- Han BC, Yun HD, Chung SY (2001) Shear capacity of reinforced concrete beams made with recycled aggregate. *ACI Special Publication* 200: 503-515.
- Mukai T, Kikuchi M (1988) Properties of reinforced concrete beams containing recycled aggregate. In: Y. Kasai, Editor, P of 2nd International RILEM Symposium on Demolition and Reuse of Concrete and Masonry, Tokyo 2: 670-679.
- Choi HB, Yi CK, Choi HH, Kang KI (2010) Experimental study on the shear strength of recycled aggregate concrete beams. *Magazine Concrete Res* 62: 103-114.
- Andrzej B, Ajdukiewicz A, Kliszczewicz T (2007) Comparative tests of beams and columns made of recycled aggregate concrete and natural aggregate concrete. *J Advanced Concrete Technol* 5: 259-273.
- Valeria C, Giacomo M (2006) Behavior of Beam-Column Joints Made of Sustainable Concrete under Cyclic Loading. *J Mat Civ Eng* 18: 50-658.
- Jianzhuan X, Yuedong S, Falkner H (2006) Seismic performance of frame structures with recycled aggregate concrete. *Eng Struct* 28: 1-8.
- Poon CS, Shui ZH, Lam L (2004) Effect of microstructure of ITZ on compressive strength of concrete with recycled aggregates. *Construct Build Mater* 18: 461-468.
- Etxeberria M, Vázquez E, Marí A (2006) Microstructure Analysis of Hardened Recycled Aggregate Concrete. *Magazine Concrete Res* 58: 683-690.
- Richart FE, Brandtzeag A, Brown RL (1928) A study of the failure of concrete under combined compressive strength, Bulletin 185, Univ. of Illinois Engineering Experimental Station, Champaign, Ill.
- ACI Committee 318, Building code requirement for reinforced concrete and commentary (ACI 319-89, ACI319R-89). American Concrete Institute, Detroit, Mich (1989).
- Mander JB, Priestley MJN, Park R (1988(b)) Theoretical Stress-Strain Model for Confined Concrete. *J Struct Div ASCE* 114: 1804-1826.
- Touahamia M, Sivakumar V, McKelvey D (2002) Shear strength of reinforced-recycled material. *Construct Build Mater* 16: 331-339.
- Stephen J. Foster (2001) On Behavior of High-Strength Concrete Columns: Cover Spalling, Steel Fibers, and Ductility. *ACI Struct J* 98: 83-589.
- Choi HB, Kang KI (2008) Bond behaviour of deformed bars embedded in RAC. *Magazine Concrete Res* 60: 399-410.
- Topcu IB (1995) Nedim Fuat GUNCAN, Using waste concrete as aggregate. *Cement Concrete Res* 25: 1385-1390.
- Choi HB (2010) Recycled aggregate-Paste interaction mechanism by Micro-structure analysis. PhD thesis, Korea University, Seoul, Korea.
- Nagataki S, Gokce A, Saeki T, Hisada M (2004) Assessment of recycling process induced damage sensitivity of recycled aggregate concrete aggregates. *Cement Concrete Res* 34: 965-971.
- Van Mier JGM (1986) Fracture of Concrete under Complex Stress, HERON, Delft University of Technology, Netherlands.
- Shah SP, Ahmad SH (1994) High Performance Concrete: Properties and Applications. McGraw-Hill, Inc.
- El-Dash KM, Mohamed RO (2006) Effect of aggregate on the performance of confined concrete. *Cement Concrete Res* 36: 599-605.